

ARTICLE

A Velocity Map Ion-imaging Study on Ketene Photodissociation at 218 nm

Jie Liu, Feng-yan Wang, Hua Wang, Bo Jiang, Xue-ming Yang*

State Key Laboratory of Molecular Reaction Dynamics, Dalian Institute of Chemical Physics, Chinese Academy of Sciences, Dalian 116023, China

(Dated: Received on November 26, 2004; Accepted on April 26, 2005)

Photodissociation dynamics of ketene at 218 nm has been investigated using the velocity map ion-imaging method. Both angular and translational energy distributions for the CO products at different rotational and vibrational states have been obtained. The 2+1 REMPI spectrum of CO products is also obtained. The results are as follows: (i) CO products in the first two vibrational states ($v''=0$ and $v''=1$) exhibit significant rotational excitation. Furthermore the rotational excitation of CO at the $v''=0$ level is noticeably higher than that at the $v''=1$ level. (ii) It was found that the major photodissociation pathway of ketene at 218 nm is the $\text{CH}_2(\tilde{a}^1\text{A}_1)+\text{CO}(X^1\Sigma^+)$ channel, while the $\text{CH}_2(\tilde{b}^1\text{B}_1)+\text{CO}(X^1\Sigma^+)$ channel and the $\text{CH}_2(\tilde{X}^3\text{B}_1)+\text{CO}(X^1\Sigma^+)$ channel are also likely present. (iii) The anisotropy parameters β of CO different rovibronic states all appear to be larger than zero. No significant difference is observed at the two vibrational states.

Key words: Velocity map ion-imaging, Photodissociation, Anisotropy parameter, Translational energy distribution

I. INTRODUCTION

Ketene has been extensively studied because of its importance in interstellar space [1, 2], and the use as a photolytical source of methylene (CH_2) radicals in both their ground ($\tilde{X}^3\text{B}_1$) and first excited ($\tilde{a}^1\text{A}_1$) electronic states. The electronic absorption spectrum of ketene has been investigated in detail previously. The electronic spectra show a long progression of apparently diffuse bands spanning the region 260–470 nm, which is assigned by Keller as the transition from the ground state to the $^1\text{A}_2$ excited state [3]. The $^3\text{A}_2$ state was estimated to be 0.25 eV below the $^1\text{A}_2$ state. For Rydberg transitions of ketene in the far-UV and vacuum-UV, the diffuse bands between 190 and 220 nm are attributed to the vibronic bands of the $\tilde{X}^1\text{A}_1 \rightarrow \tilde{B}^1\text{B}_1$ [4], which have been assigned to members of both the 3_0^n or 4_0^n progressions ($n = 1 - 3$) [5, 6], where ν_3 and ν_4 are the CH_2 scissor and $\text{C}=\text{C}$ stretching vibrations respectively. While a recent comparison of the corresponding features in the ultraviolet absorption spectra of both CH_2CO and CD_2CO suggests that the $\text{C}=\text{O}$ stretching ν_2 mode is also a major active mode for the ns Rydberg series [7].

Most of the previous studies of the dissociation dynamics of ketene concentrated on the dissociation from $^1\text{A}_2$ and $^3\text{A}_2$ excited states following excitation between 300–360 nm [8–12]. The triplet state $^3\text{A}_2$ correlates to $\text{CH}_2(\tilde{X}^3\text{B}_1)+\text{CO}(X^1\Sigma^+)$ products with a threshold of 28250 cm^{-1} above the zero point energy of the ground state of ketene molecule. It has a barrier to dissociation, which is about 1280 cm^{-1} above the dissociation limits. The singlet ground state correlates to $\text{CH}_2(\tilde{a}^1\text{A}_1)+\text{CO}(X^1\Sigma^+)$ products 3147 cm^{-1} above the triplet products. It has no energy barrier above its

asymptote. The relative yields of singlet *vs.* triplet channels have been measured as a function of the excess energy above the dissociation threshold. This measurement has been used as a benchmark to probe the quantized transition states at the barrier.

Ketene photolysis in the far-ultraviolet is less studied than the experimental work above 300 nm. Fujimoto *et al.* revealed that the CO products of 193 nm photolysis of ketene are both rotationally and vibrationally excited [13]. The evidence for the production of ketylenyl radical from photolysis of ketene at 193 nm is observed by Unfried *et al.* [14]. The $\text{CH}_2(\tilde{b}^1\text{B}_1)+\text{CO}(X^1\Sigma^+)$ channel from ketene photolysis at 212.5 nm is also detected [15]. Recently, the H atom products arising from the photodissociation of ketene in the wavelength range of 193–215 nm have been investigated by the Rydberg H atom photofragment translational spectroscopy [16]. The observed product energy disposal is interpreted in terms of one photon absorption to the $^1\text{B}_1$ excited state, internal conversion to high lying vibrational levels of the ground state and subsequently unimolecular decay. In a very recent study, we have investigated the photodissociation of ketene at 208 and 213 nm, in which rotational dependence of the product has been observed [17]. The observed phenomenon has been attributed to the photodissociation at the $\tilde{B}^1\text{B}_1$ state through a peculiar conical intersection.

The present work attempts to gain more information about the dissociation dynamics on the CH_2+CO dissociation pathways at 218 nm, which is near the threshold of excitation to the singlet $\tilde{B}^1\text{B}_1$ state. Both the angular distribution and translational energy distribution of the CO products following ketene excitation at 218 nm have been obtained.

II. EXPERIMENTAL

The experimental system was similar to that described in [18]. Sample of 5% ketene/He mixture at the

* Author to whom correspondence should be addressed. E-mail: xmyang@dicp.ac.cn

stagnation pressure of 202 kPa was expanded into a vacuum chamber through a pulsed valve (General Valve). The molecular beam passing through a skimmer was then intercepted by two pulsed, counter-propagating focused, linearly polarized laser beams, which are produced by frequency-doubling the output from two nanosecond dye lasers (Lambda Physik LPD3002E and Lambda Physik FL2002) pumped by a XeCl excimer laser (Lambda Physik LPX200). One beam photolyzed the parent molecule and the other beam probed the photofragment CO. The CO^+ ions produced by $B^1\Sigma^+ \leftarrow X^1\Sigma^+$ (2+1) resonance enhanced multiphoton ionization (REMPI) [19] were accelerated and projected onto a dual microchannel plate (MCP) detector backed by a phosphor screen. A high voltage pulse 200 ns in duration was applied to the MCP to gate the CO^+ . The transient image on the phosphor screen was captured by a thermoelectrically cooled charge-coupled-device (CCD) camera and accumulated on the CCD chip for 20000 laser shots. Simultaneously, the total emission from the phosphor screen is recorded by a photo-multiplier, and displayed on an oscilloscope. This is especially useful for signal optimization and monitoring during image data acquisition. The CO REMPI spectrum was recorded by sending the signals from the photo-multiplier to a boxcar-PC data acquisition system, scanning the laser wavelength over the two-photon resonance $\text{CO} (B^1\Sigma^+ \leftarrow X^1\Sigma^+)$. In order to measure photofragment image of the CO product in each rotational state, the laser wavelength was scanned around a single rotational line of CO to cover the entire Doppler width. The observed images of CO^+ were two-dimensional (2D) projections of the original three-dimensional (3D) CO product scattering distributions. Since the CO spatial distributions were cylindrically symmetric around the electric vector of the laser beam, the sections of the 3D distributions were reconstructed by inverse Abel transformations.

Ketene was prepared by thermal decomposition of acetic anhydride in a quartz oven at 650 °C, and purified by distilling 3 times from 196 to 77 K [10].

III. RESULTS

A. CO REMPI spectrum

Ketene was photodissociated at the photolysis laser wavelength of 218.07 nm. The CO fragment was detected by 2+1 REMPI via the Q-branch of the $B^1\Sigma^+ \leftarrow X^1\Sigma^+$ transition at 230.1 nm. This transition is free from alignment effects [20], and simplifies the interpretation of the derived anisotropy parameters. In Fig.1, the REMPI spectrum of the CO photofragment is shown. The Q-branches of the vibrational transitions $v''=0 \rightarrow v'=0$ and $v''=1 \rightarrow v'=1$ are observed. Rotational transitions up to $J''=74$ in $v''=0$ and $J''=45$ in $v''=1$ can be clearly assigned. The $\text{CO}(B^1\Sigma^+, v=0)$ state is weakly predissociative for $J \geq 38$ [21], Rottke and Zacharias have reported that the predissociation is J-independent [22]. The sharp decrease in the line intensity for the $v'=1$, $J=18$ and $J=36$ lines are also

observed, which are due to the $\text{CO}(B^1\Sigma^+)$ predissociation [23]. From the REMPI spectrum, CO products in spectrum, CO products in the first two vibrational states ($v''=0$ and $v''=1$) exhibit significant rotational excitation. Furthermore the rotational excitation of CO at the $v''=0$ level is noticeably higher than that at the $v''=1$ level.

B. $\text{CO}(X^1\Sigma^+)$ product translational energy distribution

Shown in Fig.2 are the cuts of the inverse Abel transformed images from the raw image data obtained in this experiment at excitation laser wavelength 218.07 nm

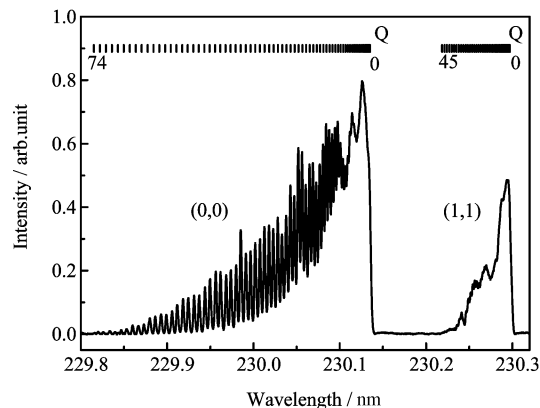


FIG. 1 2+1 REMPI spectrum of $\text{CO} (B^1\Sigma^+ \leftarrow X^1\Sigma^+)$, obtained by photodissociating ketene at 218.07 nm

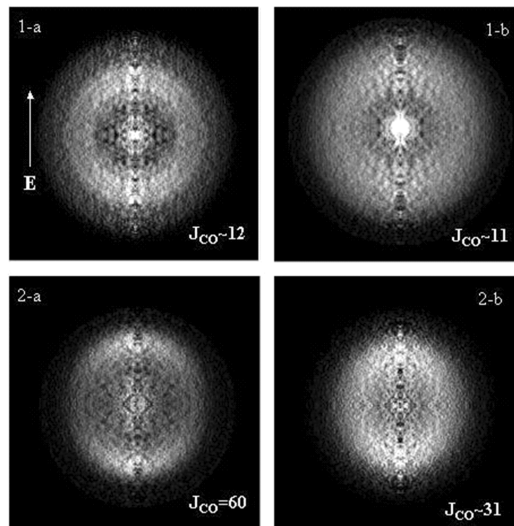


FIG. 2 Inverse Abel transforms of the $\text{CO} (X^1\Sigma^+)$ images of ketene photodissociated at 218.07 nm for selected rotational levels of the $v''=0$ (panels 1-a and 2-a) and $v''=1$ (panels 1-b and 2-b) vibrational states. The arrows indicate the polarization direction of the laser.

for the selected rotational levels of the CO products at the $v''=0$ and $v''=1$ vibrational levels. Panels 1-a and 2-a show the cuts of inverse Abel transformed images at the $v''=0$ vibrational level, while panels 1-b and 2-b show the cuts of inverse Abel transformed

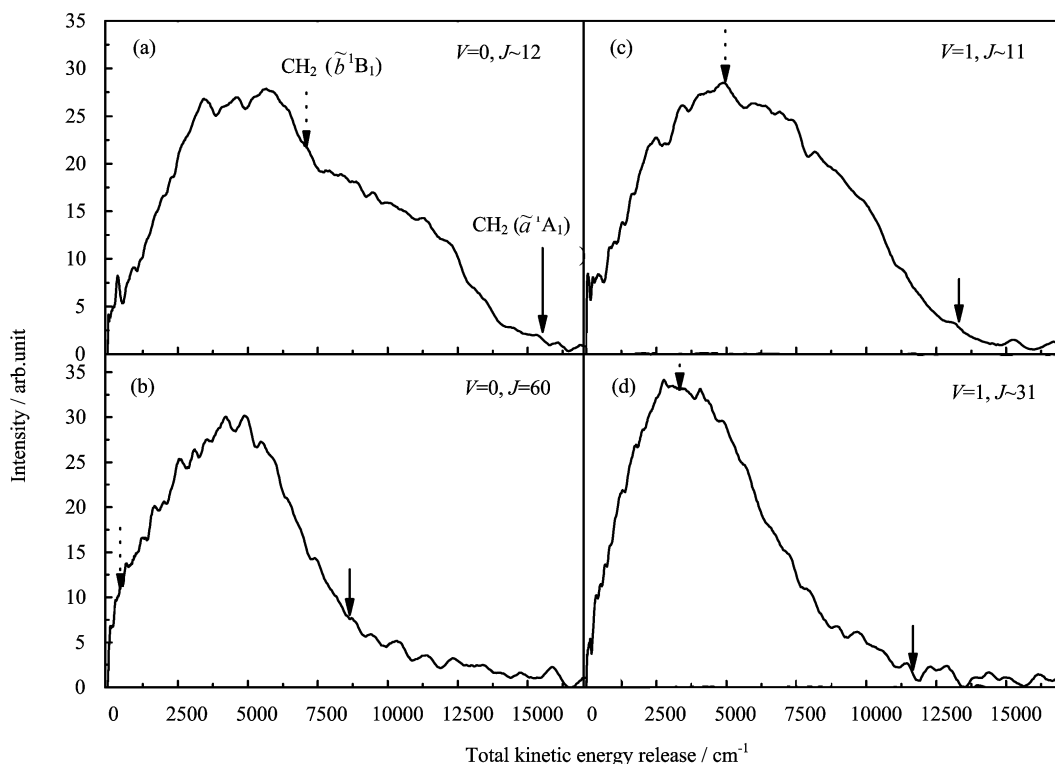


FIG. 3 Product translational energy distributions for photodissociation of ketene at 218.07 nm of $v''=0$ and $v''=1$ vibrational states for selected rotational levels of CO fragment: (a) $v''=0$, $J''_{\text{CO}}\sim 12$, (b) $v''=0$, $J''_{\text{CO}}=60$, (c) $v''=1$, $J''_{\text{CO}}\sim 11$, (d) $v''=1$, $J''_{\text{CO}}\sim 31$. The solid arrow indicates the maximum kinetic energy possible for producing $\text{CH}_2(\tilde{a}^1A_1)$ fragments, and the dashed arrow indicates the maximum kinetic energy possible for producing $\text{CH}_2(\tilde{b}^1B_1)$ fragments in each panel.

images at the $v''=1$ vibrational level. By accumulating signals in each panel of Fig.2 at different velocities, the product velocity distribution and thus the translational energy distribution could be derived. Figure 3 shows the product translational energy distributions of ketene at both vibrational states for selected rotational levels. In each panel, the solid arrow indicates the maximum kinetic energy possible for producing the $\text{CH}_2(\tilde{a}^1A_1)$ fragments, and the dashed arrow indicates the maximum kinetic energy release possible for producing $\text{CH}_2(\tilde{b}^1B_1)$ fragments. Most of the products are produced with low translational energy peaking at total kinetic energy $\sim 4500\text{ cm}^{-1}$. The low release translational energy indicates that the dissociation is indirect. Since the rotational excitation of the CO product is quite high, the CH_2 fragment should also likely have significant rotational excitation due to angular momentum conservation. This argument is consistent with the observation that no clear vibrational structures of the CH_2 fragment are observed in the translational energy distributions, suggesting the rotational excitation of the CH_2 product should be quite high. From Fig.3, most of the CO products at $v''=0$, $J''=60$ rotational state are observed with translational energy above the \tilde{b}^1B_1 energetic limit. Therefore, we believe that most of the CH_2 products should be mainly in the \tilde{a}^1A_1 state, which is in agreement with the previous experimental study [16]. There still exist some products with kinetic energy exceeding the maximum kinetic en-

ergy release possible for producing the $\text{CH}_2(\tilde{a}^1A_1)$ fragments. One possible source of these products is from the $\text{CH}_2(\tilde{X}^3B_1)+\text{CO}(X^1\Sigma^+)$ channel. The existence of this channel would be consistent with its absence at low J states, since triplet CH_2 is very unlikely present at low J states [24]. In Fig.3 panel (a), a peak appears at $\sim 300\text{ cm}^{-1}$ when the CO product is at low rotational state $J''\sim 12$. From the energetic limit consideration, it is believed that this feature is due to the formation of $\text{CH}_2(\tilde{b}^1B_1)$ fragments. Similar feature is also observed at $v''=1$ at the low rotational state $J''\sim 11$ (Fig.3 panel 3-c), indicating this feature is only correlated to the low rotational excited CO product. It should be noted that this channel is a minor process.

C. CO ($X^1\Sigma^+$) product angular distribution

From Fig.2 the product angular distributions could also be determined. This distribution can be fitted using the standard recoil anisotropy function [25], $I(\theta)=I_0[1+\beta(3/2\cos^2\theta-1/2)]$. In the above equation, θ is the angle between the polarization vector of the photolysis laser and the velocity vector v and β is the spatial anisotropy parameters. CO product angular distribution for photodissociation of ketene at 218.07 nm for the $v''=0$, $J''=60$ rotational state is shown in Fig.4. Figure 5 shows the anisotropy parameters β determined for each rotational J'' state in photodissocia-

tion of ketene at 218.07 nm of the $v''=0$ and $v''=1$ vibrational states. the anisotropy parameters β all appear to be larger than zero, indicating that the dissociation should be a quite fast process. No significant difference is observed for the CO products at the two vibrational states.

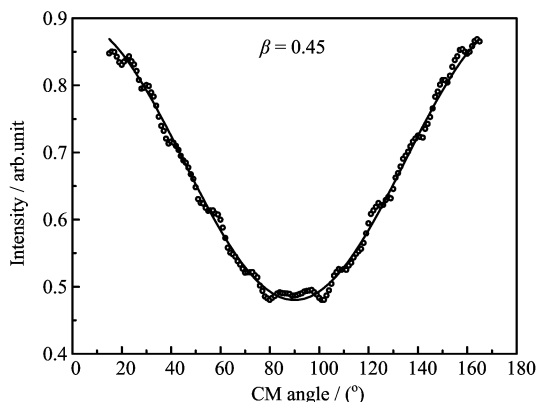


FIG. 4 CO products angular distribution for photodissociation of ketene at 218.07 nm for the $v''=0$, $J''_{CO}=60$ rotational level. Solid curves represent the least-squares fittings to the equation $I(\theta) = I_0[1 + \beta(3/2 \cos^2 \theta - 1/2)]$

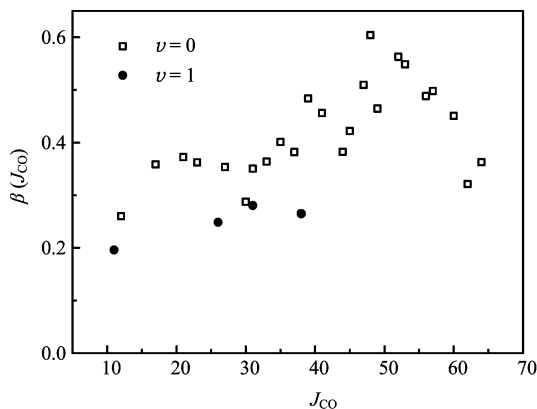


FIG. 5 Rotational dependence of anisotropy parameters (β) of CO ($X^1\Sigma^+$) products in photodissociation of ketene at 218.07 nm. The errors in each β value were estimated to be smaller than ± 0.08 .

IV. DISCUSSION

As a model system for unimolecular dissociation, extensive theoretical studies on ketene photodissociation have been carried out previously. *Ab initio* studies by Allen and Schaefer [26–28] found that both C_{5v} -I and C_{2v} dissociation pathways are symmetry allowed for the 1B_1 state ketene. In the C_{5v} -I [26], the 1B_1 state correlates to $CH_2(\tilde{b}^1B_1)+CO(X^1\Sigma^+)$ and the 3A_1 state which crosses the 3A_2 state correlates to $CH_2(\tilde{X}^3B_1)+CO(X^1\Sigma^+)$ products. More theoretical studies [5] show that C_{2v} symmetry is broken upon bending of the CCO angle when the 1B_1 state stabilizes, indicating C_{5v} -I dissociation pathway is dynamically more likely than the C_{2v} dissociation route. The

translational energy distribution observed in this experiment indicates that direct dissociation along the C_{5v} -I pathway producing $CH_2(\tilde{b}^1B_1)+CO(X^1\Sigma^+)$ products is a minor dissociation channel. The major dissociation pathway is the production of $CH_2(\tilde{a}^1A_1)+CO(X^1\Sigma^+)$ via either $\tilde{B}^1B_1 \rightarrow \tilde{X}^1A_1$ or $\tilde{B}^1B_1 \rightarrow \tilde{A}^1A_2 \rightarrow \tilde{X}^1A_1$ decay. Rotational dependence of the CO product angular anisotropy has been observed for the ketene photodissociation at 208 and 213 [17]. In which the excitation of these two wavelengths are all through two clear vibronic bands of the $\tilde{X}^1A_1 \rightarrow \tilde{B}^1B_1$ transition. The observation of the rotational dependence of the product angular anisotropy is an indication that the dissociation processes at these two wavelengths should go through a peculiar conical intersection, which could produce such interesting dynamical feature as in the H_2O [29] and NH_3 [30] photodissociation. Obviously, no such clear rotational dependence of the CO product angular anisotropy has been observed at the 218 nm wavelength. The excitation of ketene at 218 nm is far away from the 213 nm band. Therefore the electronic character of the excited ketene at 218 nm excitation should be significantly different from that at 213 nm excitation. It is possible that the main character of the excitation at 218 nm is through a direct repulsive state, which correlates to the ground singlet surface. This could explain the dynamical difference between the 208/213 nm result and the 218 nm result. Even though the rotational dependence of the CO product angular anisotropy at 218 nm excitation is not as obvious as in the 208/213 nm excitation, there still some rotational dependence, indicating that the dynamics producing the high rotationally excited CO product might be different from that producing the low rotationally excited CO product. The minor $CH_2(\tilde{X}^3B_1)+CO(X^1\Sigma^+)$ channel has also been observed in this excitation wavelength, which could occur through the $\tilde{B}^1B_1 \rightarrow ^3A_1$ internal conversion along the C_{5v} -I dissociation pathway.

V. CONCLUSION

Ketene photodissociation at the 218 nm excitation have been investigated using the velocity map ion-imaging technique. Both angular and translational energy distributions for the CO products at different rotational and vibrational states have been determined. The $CH_2(\tilde{a}^1A_1)+CO(X^1\Sigma^+)$ channel is found to be the main dissociation process, while the $CH_2(\tilde{b}^1B_1)+CO(X^1\Sigma^+)$ channel and the $CH_2(\tilde{X}^3B_1)+CO(X^1\Sigma^+)$ channel are also likely present. The experimental results here are then compared with that at the 208/213 nm, suggesting that ketene photodissociation mechanism at 218 nm excitation is significantly different from that at 208/213 nm excitation.

VI. ACKNOWLEDGMENT

This work is supported by the Chinese Academy of Sciences, the Ministry of Science and Technology, and

the National Natural Science Foundation of China.

- [1] J. M. Hollis, R. D. Suenram, F. J. Lovas and L. E. Snyder, *Astron. Astrophys.* **126**, 393 (1983).
- [2] H. E. Matthews and T. J. Sears, *Astrophys. J.* **300**, 766 (1986).
- [3] A. H. Laufer and R. A. Keller, *J. Am. Chem. Soc.* **93**, 61 (1971).
- [4] O. Berg and G. E. Ewing, *J. Phys. Chem.* **95**, 2908 (1991).
- [5] P. G. Szalay, A. G. Csaszar and L. Nemes, *J. Chem. Phys.* **105**, 1034 (1996).
- [6] M. B. Robin, *Higher Excited States of polyatomic Molecules*, Academic Orlando, 1985. Vol. 3
- [7] S. Y. Chiang, M. Bahou, Y. J. Wu and Y. P. Lee, *J. Chem. Phys.* **117**, 4306 (2002).
- [8] I. C. Chen, W. H. Green, Jr. C. B. Moore, *J. Chem. Phys.* **89**, 314 (1988).
- [9] I. C. Chen, C. B. Moore, *J. Phys. Chem.* **94**, 269 (1990).
- [10] S.K. Kim, Y. S. Choi, C. D. Pibel, Q. K. Zheng and C. B. Moore, *J. Chem. Phys.* **94**, 1954 (1991).
- [11] I. G. Moreno, E. R. Lovejoy and C. B. Moore, *J. Chem. Phys.* **100**, 8902 (1994).
- [12] S. K. Kim, E. R. Lovejoy and C. B. Moore, *J. Chem. Phys.* **102**, 3202 (1995).
- [13] G. T. Fujimoto, M. E. Umstead and M. C. Lin, *Chem. Phys.* **65**, 197 (1982).
- [14] K. G. Unfried, G. P. Glass and R. F. Curl, *Chem. Phys. Lett.* **177**, 33 (1991).
- [15] M. Castillejo, M. Martin, R. de Nalda, M. Oujja, *Chem. Phys. Lett.* **237**, 367 (1995).
- [16] E. J. Felthan, R. H. Qadiri, E. E. H. Cottrill, P. A. Cook, J. P. Cole, G. G. Balint-Kurti and M. N. R. Ashfold, *J. Chem. Phys.* **119**, 6017 (2003).
- [17] J. Liu, F. Y. Wang, H. Wang, B. Jiang and X. M. Yang, *J. Chem. Phys.* **122**, 104309 (2005).
- [18] A. T. J. B. Eppink and D. H. Parker, *Rec. Sci. Instrum.* **68**, 3477 (1997).
- [19] P. J. H. Tjossem and K. C. Smyth, *J. Chem. Phys.* **91**, 2041 (1989).
- [20] Th. Droz-Georget, M. Zyrianov, H. Reisler and D. W. Chandler, *Chem. Phys. Lett.* **276**, 316 (1997).
- [21] G. W. Loge, J. J. Tiee and F. B. Wampler, *J. Chem. Phys.* **79**, 196 (1983).
- [22] H. Rottke and H. Zacharias, *Opt. Commun.* **55**, 87 (1985).
- [23] W. L. Tchchang-Brillet, P. S. Julienne, J. M. Robbe, C. Letzelter and F. Rostas, *J. Chem. Phys.* **96**, 6735 (1992).
- [24] C. G. Morgan, M. Drabbels, A. M. Wodtke, *J. Chem. Phys.* **104**, 7460 (1996).
- [25] R. N. Zare, *Mol. Photochem.* **4**, 1 (1972).
- [26] W. D. Allen and H. F. Schaefer III, *J. Chem. Phys.* **84**, 2212 (1986).
- [27] W. D. Allen and H. F. Schaefer III, *J. Chem. Phys.* **87**, 7076 (1987).
- [28] W. D. Allen and H. F. Schaefer III, *J. Chem. Phys.* **89**, 329 (1988).
- [29] S. A. Harich, D. W. H. Huang, X. F. Yang, J. J. Lin, X. Yang, and R. N. Dixon, *J. Chem. Phys.* **113**, 10073 (2000).
- [30] D. H. Mordaunt, M. N. R. Ashfold and R. N. Dixon, *J. Chem. Phys.* **104**, 6460 (1996).